Measuring the Fermi energy of aluminium with electron-positron annihilation

University of Technology, Delft
Daniël Bouman & Kenneth Goodenough
Student number: 4146077 & 4334175
D.Bouman@student.tudelft.nl & K.D.Goodenough@student.tudelft.nl

1. Introduction

The Fermi energy of a material is the difference between the highest and lowest electron-energies of the material at $T = 0$ K. The goal of this research project is to measure the Fermi energy of aluminium, using a commonly applied method called the Angular Correlation of Annihilation Radiation (ACAR) [1]. ACAR relies on the fact that the angle between the two photons that are created during electron-positron annihilation is a measure for the momentum of the electron prior to the annihilation process. Since the Fermi energy of a material dictates the maximum momentum of the electron, the minimum angle found between the two photons is a measure for the Fermi energy. For this research project, a ^{22}Na source was used which emits positrons that annihilated primarily with the free electrons in the aluminum surrounding the source. Two scintillation detectors were positioned on opposite sides of the source. The angle between the two detectors was varied and for each angle the number of simultaneous photons was counted. A theoretical curve was fitted to the measured data, from which the Fermi energy was calculated.

2. Theory

When a positron (β^+) collides with an electron (e^-), which is the antiparticle of a positron, electron-positron annihilation will occur. For collisions at low energy, the most common case involves the creation of two gamma ray photons (γ):

$$e^- + \beta^+ = \gamma + \gamma. \tag{1}$$

The total process should obey the laws of conservation of energy and momentum, therefore two photons are created as opposed to one photon. For one photon, total momentum and energy cannot be conserved in this process. Assuming that the momentum of the positron and electron combined before the collision is zero, the two photons will have trajectories in exactly opposite directions to conserve momentum. The rest energy of the positron and electron is equally distributed over the two photons, i.e. the photons both have energy $m_0c^2 \approx$ 511 keV. In practice, the momentum of the positron and electron is never zero, resulting in small deviations in the angle between the two photons and the energy of 511 keV. In a dense material, such as aluminium, the positron will lose most of its momentum due to collisions. Thus, assuming that the positron has zero momentum before annihilating with an electron with non-zero momentum $\boldsymbol{p}$, the deviations will be indicative of the momentum of the electron before the collision. From the formula for Fermi-Dirac statistics:

$$f(E) = \frac{1}{e^{\frac{(E-E_F)}{kT}} + 1}, \tag{2}$$

where $f(E)$ is the probability for a fermion to have energy E, E_F the Fermi energy, k the Boltzmann constant and T the temperature [1]. From this equation it follows that there is a maximum energy that can be occupied by the electrons at $T = 0$ K, namely the Fermi energy E_F. Energies between 0 and E_F all have an equal chance of being occupied. For $T \approx 300$ K the Fermi energy is still an acceptable measure for the maximum energy of the electrons in metal, since $E_F \gg kT$ when $T = 300$ K and E_F is order of magnitude 10 eV, which is an estimate for the Fermi energy in a metal [2]. The maximum

[1] For a derivation, see for example Griffiths' book *Introduction to Quantum Mechanics*, Prentice Hall

momentum associated with the Fermi energy is called the Fermi momentum $\boldsymbol{p_F}$ and the length is defined naturally then as $p_F = \sqrt{2mE_F}$.

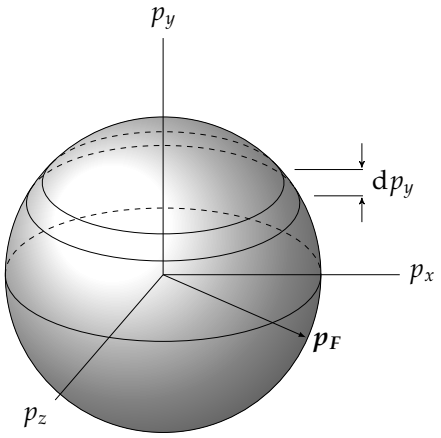

Figure 1: *Infinitesimal slice of a sphere with radius* $\boldsymbol{p_F}$

Let $\boldsymbol{p_e}$ denote the momentum vector of an electron and $\boldsymbol{p_y}$ the y-component of $\boldsymbol{p_e}$. The relation between the difference in the angle and the momentum of the electron can be derived (see appendix A):

$$\theta = \frac{p_y}{m_e c}. \tag{3}$$

Since the maximum magnitude of the $\boldsymbol{p_e}$ vector is fixed via the Fermi momentum and the possible directions of $\boldsymbol{p_e}$ are equally distributed over all angles, the total possible $\boldsymbol{p_e}$ vectors are given by a ball with radius p_F, see figure 1. Assuming that all magnitudes of p_e are equally likely, the chance that positron-electron annihilation will occur with an electron with $\boldsymbol{p_y}$ having a value lying between p_y and $p_y + dy$ is proportional to the volume of the disk-segment between two points p_y and $p_y + dx$. The volume of such a disk-segment is given by $4\pi p_r^2 = 4\pi(p_F^2 - p_y^2)dx$. The chance is thus proportional to $p_F^2 - p_y^2$, which forms a parabola. Since this chance is directly proportional to the measured angles, the minimum angle, denoted as the Fermi angle θ_F, between two photons will occur when $||\boldsymbol{p_y}|| = ||\boldsymbol{p_F}||$. Then from equation 3 it follows that $||\boldsymbol{p_F}|| = m_e c\theta_F = \sqrt{2m_e E_F}$, and so:

$$E_F = \frac{m_e c^2 \theta_F^2}{2}. \tag{4}$$

However, the positrons will also annihilate with bound electrons, resulting in an additional Gaussian distribution in addition to the angle correlation.

3. Experimental Setup

In this experiment a ^{22}Na is used as a positron source (details about ^{22}Na are discussed in Appendix B) and is positioned in between two scintillation detectors, both equipped with a photomultiplier tube (PMT) and an amplifier. Due to the source emitting primarily positrons, positron-electron annihilation will occur in the surrounding aluminium. The scintillation detectors allow detection of the γ-radiation resulting from electron-positron annihilations. A motorized stage is used to displace one of the scintillation detectors over a small angle, allowing measurements across an angular range. Computer software is used to control the stage and acquire the data corresponding to the angles. Using an array of electronics only simultaneous 511 keV photons are registered. Over a period of five days the data is collected. The data is then fit to a fitting function with several parameters.

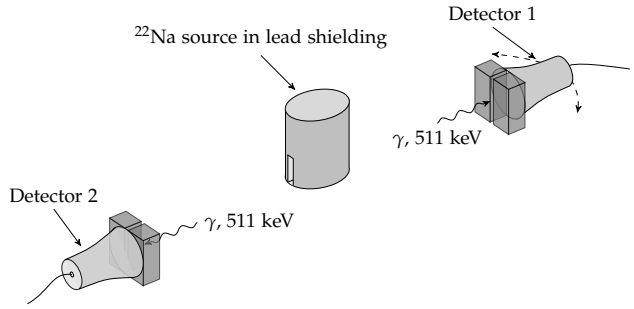

Figure 2: *Experimental setup. The source and Al sample are enclosed by lead shielding with exit slits towards the detectors. Collimators are used to shield the detectors from photons with incident angles other than perpendicular to the detector surface. Detector 1 can be rotated along the dashed lines.*

^{22}Na source and scintillation detectors

The ^{22}Na source is deposited on an aluminium substrate through physical vapor deposition and on top of this another piece of aluminum is placed, enclosing the ^{22}Na source. The aluminium substrate is then encapsulated in a solid plastic cylinder, to prevent direct exposure of the source.

High-energy photons from the positron-electron annihilation can propagate through two slits on opposite sides of the lead shielding around the source (Figure

2). Photons which are not incident perpendicular with respect to the detector surface are absorbed by lead collimators in front of the scintillator detectors. Since the collimators have a non-zero width, the photons that are measured still have a small range of incident angles. Since one slit acts as rectangular spatial filter, two slits give a triangular function through convolution of the two rectangular functions. Convolution with the fitting function will better approximate the measured data.

The remaining photons that are incident on the scintillator will excite electrons from the scintillator material and lose energy for each excitation. The excited electrons will fall back to a lower energy state, emitting low-energy photons in the process. The amount of photons is proportional to the energy of the initial incident photon. These photons are incident on a photo-cathode inside the PMT which is coupled to the scintillation crystal. Through the photo-electric effect, the low-energy photons will free electrons on from the cathode. The number of freed electrons is proportional to the amount of absorbed low-energy photons, and thus proportional to the energy of the initial incident high-energy photon. Further, the photo-cathode is a thin sheet, which would allow a high-energy photon to pass through the cathode and possibly not free any electrons at all.

The PMT also contains an array of dynodes, which acts as an electron multiplier. The dynodes have a large positive voltage (in the order of kV's) and each consecutive dynode has a larger voltage (around 100 V). The freed electrons are directed and focused toward the first dynode. Accelerated by the electric field due to the potential difference, the electrons arrive each with a kinetic energy of around 100 eV. Upon striking the dynode more electrons are freed. The electrons are then accelerated towards the second dynode where the same process starts again. The arrangement of the dynodes is such that a cascade occurs where at each dynode the number of electrons increases. At the end of the tube the electrons reach the anode, where the electrons produce a sharp current pulse proportional to the energy of the incident photon.

For the angle dependent measurements, detector 1 can be rotated around a range of angles (Figure 2). The detector is rotated with a stepping motor, controlled by the measurement software.

Signal processing

The pulse from the PMT attached to detector 1 is acquired by a single channel analyser (SCA). When the SCA recognizes a current from the PMT, it sends a logical pulse to a time-to-amplitude converter (TAC), which starts a 200 ns timer upon receiving this pulse. If a pulse from detector 2 is received within a certain time frame, a signal is sent to an analog-to-digital converter (ADC). The ADC sends a signal to the computer which registers this as an annihilation event corresponding to the current angle of detector 1.

Two photons from an annihilation process will arrive at the detectors at roughly the same time. Thus to ensure that the TAC has enough time to register the pulse from detector 2 after the timer starts, a time delay between detector 2 and its SCA is created by using a significantly longer coax cable. The length is chosen such that the electromagnetic waves propagating through the dielectric insulator of the coaxial cable arrive within the 200 ns time frame. This ensures that photons from the same annihilation are measured and, because at most 1 annihilation takes place every microsecond (source activity at the moment of experiment is approximately 1 MBq), photons from different annihilation events are excluded.

The detectors are not only sensitive to 511 keV photons. The 1274,5 keV γ-radiation from the ^{22}Na source as well as background radiation is also detected (see Figure 6 in appendix C for the unfiltered measured spectrum). To exclude these photons from the measurements, acquisition windows on the SCA's are calibrated to only allow 511 keV photons. Figure 7 in appendix D shows a detector histogram with only the isolated 511 keV photons.

When the ADC send a signal to the computer, the software registers this event. After an interval the software writes the number of measured annihilations in a spreadsheet with the corresponding angle. At the same time the step motor moves detector 1 to the next angle, repeating this process for the full length of the experiment.

Experiment details

Because the majority of the annihilation photons are not detected, the length of the experiment has to be relatively long. To obtain enough photons for a proper statistical analysis, the experiment ran 120.6 hours.

During this time the angle between detector 1 and the normal θ is changed by 3.3 °. At every angle data is acquired for 2160 s. The setup was calibrated using a less active positron source.

4. Results

The data of the ACAR experiment is shown in Figure 3. The shape of the curve is, as expected, a combination of a Gaussian, parabola and a convolution function, as was discussed in the previous chapters.

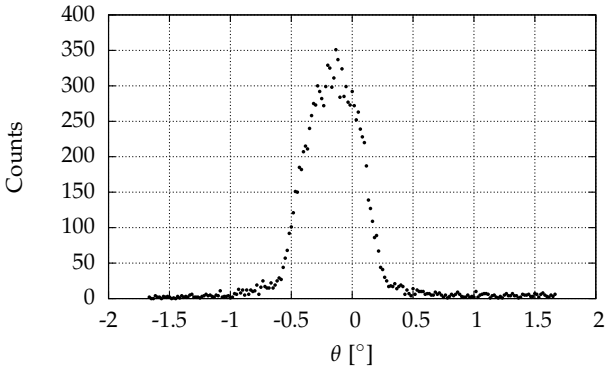

Figure 3: *Angle correlation between 511 keV annihilation photons. The angle was changed with an increment of 0.017 ° and data was acquired for 2160 s per angle. q*

To obtain the parameters that best fit the measured data, a least squares method is performed in LabVIEW by calculating the sum of the squared residuals for each combination of the parameters over a suitable range. First the plausible ranges of values for the parameters were found by hand. Taking into account desired accuracy and program runtime (the program is $O(n)$), the stepsize and amount of steps for each parameter is selected accordingly. The following values were selected:

Parameter	Start value	Step size	Steps
Fermi angle θ_F	6.65 mrad	0.01	65
Core width	5.8 mrad	0.01	20
Fraction core annihilations	0.15	0.05	8
Slitwidth	0.5 mm	0.05	20
^{22}Na source radius	0.007 mm	0.001	6
Background coincidence counts	1	0.05	20
Alignment correction	1.6	0.01	250

The collimator distance was fixed to 600 mm. A minimum for the squared and summed residuals was found when the parameters were set to:

Parameter	Value
Fermi angle θ_F	6.98 mrad
Core width	5.94 mrad
Fraction core annihilations	0.20
Slitwidth	1.10 mm
^{22}Na source radius	0.01 mm
Background coincidence counts	1.45
Alignment correction	2.73

The Fermi energy corresponding to a Fermi angle of 6.98 milliradians equals 12.46 eV. The literature value for the Fermi energy of aluminium is 11.65 eV [2, 3]. This deviation from the literature value most likely originates from the fitting process. During manual fitting it was observed that small deviations in certain parameters had a significant effect on the value for the Fermi angle that produced the lowest squared and summed residuals. Another explanation would be the inaccuracies caused by the approximation that the positron is stationary during the electron-positron annihilation process.

5. Conclusion

For this project the Fermi energy of aluminium was determined through the angular correlation of annihilation radiation. A ^{22}Na was used as a positron source, the positrons annihilate with electrons in aluminium surrounding the ^{22}Na. After fitting a function as closely as possible function to the measured, a Fermi energy of 12.46 eV was found. The discrepancy with the value

of 11.65 eV found in literature [2,3] is most likely due to errors in the fitting process.

References

[1] E. do Nascimento, O. Helene, V.R. Vanin, M.T.F. da Cruz, and M. Moralles. Statistical analysis of the doppler broadening coincidence spectrum of electron-positron annihilation radiation in silicon. *Nuclear Instruments and Methods in Physics Research Section A: Accelerators, Spectrometers, Detectors and Associated Equipment*, 609(2-3):244 – 249, 2009.

[2] N.W. Ashcroft and N.D. Mermin. *Solid state physics*. Science: Physics. Saunders College, 1976.

[3] T.B Massalski and U Mizutani. Electronic structure of hume-rothery phases. *Progress in Materials Science*, 22(3-4):164, 1978.

[4] G. Gilmore. *Practical Gamma-ray Spectroscopy*. Wiley, 2011.

[5] G. Brouwer. *Practical Radiation Protection*. Syntax Media, Arnhem, 2010.

A. Derivation of Fermi energy as function of the Fermi angle

Conservation of mass-energy gives:

$$2m_0c^2 = cp_1 + cp_2,$$

where p_1 and p_2 are the length of the corresponding momentum-vectors. If $\boldsymbol{p_e}$ has length p_e, an arbitrary angle φ with the x-axis and setting the momentum $\boldsymbol{p_1}$ of one of the photons in the x-direction the following situation occurs:

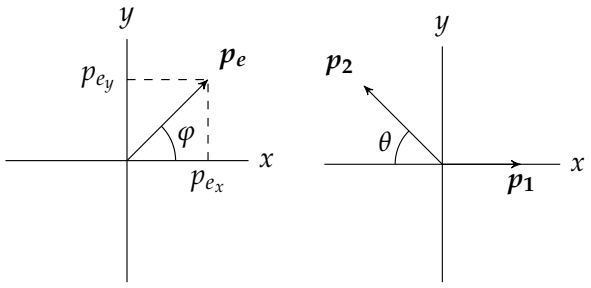

(a) *Momentum of an electron $\boldsymbol{p_e}$ with an angle φ to the x-axis*

(b) *Momentum of the two photons $\boldsymbol{p_1}$ and $\boldsymbol{p_2}$, with the direction of $\boldsymbol{p_1}$ fixed to the x-axis and $\boldsymbol{p_2}$ has an angle θ with the negative x-axis.*

Figure 4: *Schematic of the momentum-vectors of the electron and two photons, assuming the positron has no momentum during the annihilation process.*

Conservation of linear momentum implies the conservation of both the x- and y-component of the momentum, which gives the following equations:

$$\begin{aligned} p_e\cos(\varphi) &= p_1 - p_2\cos(\theta) \\ p_e\sin(\varphi) &= p_2\sin(\theta). \end{aligned}$$

From which it follows that:

$$\begin{aligned} p_2 &= p_e\frac{\sin(\varphi)}{\sin(\theta)} \\ p_1 &= p_e\cos(\theta) + p_2\cos(\theta) \\ &= p_e\cos(\theta) + p_e\cos(\theta)\frac{\sin(\varphi)}{\sin(\theta)} \\ 2m_0c^2 &= cp_1 + p_2 \\ &= cp_e\left(\cos(\theta) + \cos(\theta)\frac{\sin(\varphi)}{\sin(\theta)} + \frac{\sin(\varphi)}{\sin(\theta)}\right). \end{aligned}$$

For low energies of the electron $p_e \ll m_0c$, and from that it follows that θ is small which implies that the small-angle approximation can be used (i.e. $\sin(\theta) \approx \theta$

and $\cos(\theta) \approx 1$):

$$
\begin{aligned}
2m_0c^2 &= cp_e\left(\cos(\theta) + \cos(\theta;)\frac{\sin(\varphi)}{\sin(\theta)} + \frac{\sin(\varphi)}{\sin(\theta)}\right) \\
2m_0c &\approx p_e\left(1 + 2\frac{\sin(\varphi)}{\theta}\right) \\
&\approx p_e + \frac{2p_e\sin(\varphi)}{\theta} \\
2m_0c - p_e &= \frac{2p_e\sin(\varphi)}{\theta} \\
\theta &= \frac{2p_e\sin(\varphi)}{2m_0c - p_e} \\
\theta &\approx \frac{p_y}{m_0c}.
\end{aligned}
$$

B. Measuring the relation between channels and energy

^{22}Na decays into ^{22}Ne by different means. Most prominently (90% of the time) it will decay to the 1274 keV energy level of ^{22}Ne, emitting a 545 keV positron in the process. 10% of the time an electron will be absorbed instead of a positron being emitted. The ^{22}Ne will fall to the ground state within picoseconds by emitting 1274 keV γ-radiation. On rare occasions, 0.05% of the time, the ^{22}Na decays directly into the ^{22}Ne ground state by emitting a 1.83 MeV positron (Figure 5) [4]. A measurement of a ^{22}Na source with aluminium around it (see figure 6) shows these transitions, where the peak between 500 keV and 600 keV is from annihilation events, not from the 454 keV positrons.

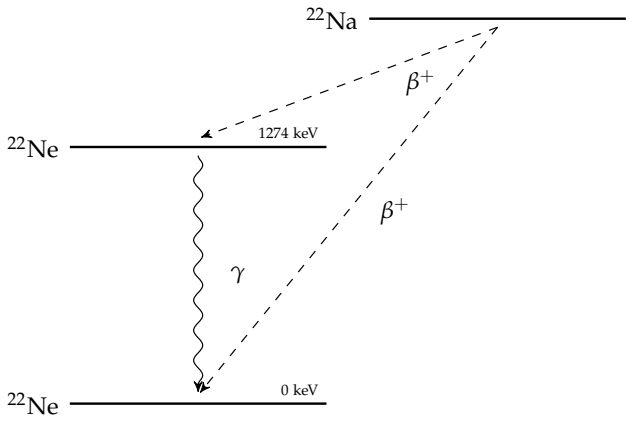

Figure 5: *Decay scheme of ^{22}Na source. A large portion (90 %) will disintegrate to the 1.275 MeV level of ^{22}Ne (545 keV β^+), which can fall to the ground state (1.275 MeV γ). A small fraction (0.05 %) will decay directly to the ^{22}Ne ground state (1.83 MeV β^+).*

The standard peak detection algorithm in MATLAB is used to find the peaks in the energy spectrum. The algorithm found two peaks at channels 1001 and 2499, corresponding to 511 keV and 1.275 MeV respectively. From this it follows that the channels and energies differ a factor 0.5105.

C. Unfiltered energy spectrum

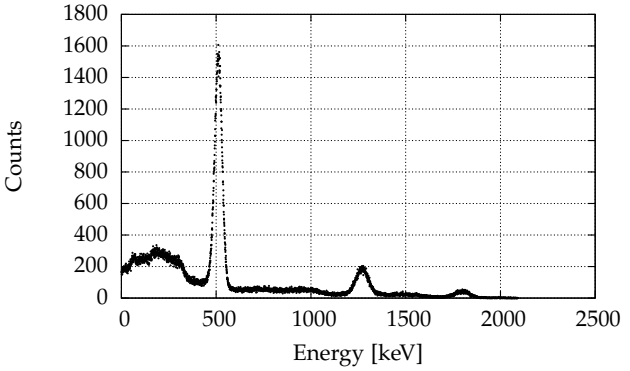

Figure 6: *Energy spectrum without acquisition windows on the SCA's. Besides the 511 keV annihilation photons, radiation from Compton scattering and the ^{22}Na isotope falling to the ground state (1274.5 keV) is present. The small peak around 1.8 MeV is due to 511 and 1274.5 keV photons being registered as one particle by the detector.*

D. Energy spectrum filtered for 511 keV photons

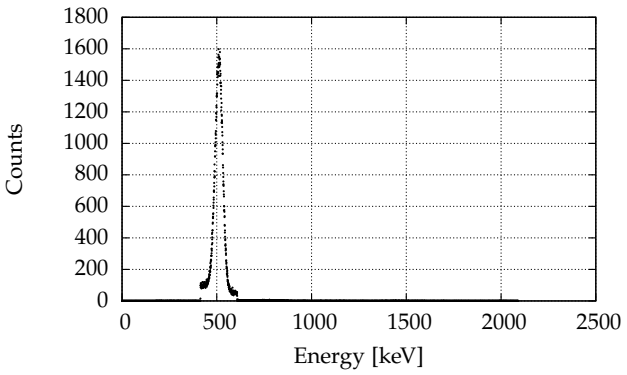

Figure 7: *Energy spectrum after calibrating the acquisition windows on the SCA's, so that only 511 keV radiation is registered.*

E. Radiation risk analysis

The equivalent dose H_T is found by multiplying the dose averaged over the tissue D with a weighting factor w_R:

$$H_T = w_R \cdot D. \tag{5}$$

The dose is measured in gray (Gy or J·kg^{-1}), for this analysis a weighting factor of 1 used, this corresponds to a full body exposure.

The dose can be found with the following equation:

$$D = \frac{\Gamma A}{r^2} e^{-\mu d} \tag{6}$$

where Γ stands for the source constant in Gy·m^2·Bq^{-1}·h^{-1}, A for the activity in Bq and r is the distance from the observer to the source in meters. μ is the total linear interaction coefficient. It is an inherent property of the shielding material and the value is obtained from literature. d is the thickness of the shielding material.

In the setup a ^{22}Na isotope is used as source. The activity was measured on July 1st 2006 to be 4 MBq. ^{22}Na has a half-life of 2.6 years, giving a current activity of

$$A = A_0 e^{-\frac{t \ln(2)}{\tau}} = 4 \cdot e^{-\frac{7.6 \ln(2)}{2.6}} \approx 0.5 \text{ MBq}.$$

When charged particles particles are slowed down by other charged particles the kinetic energy is converted to a photon. This process is called Bremsstrahlung, and occurs in the experiment when the β^+-particles are slowed by the electrons in the atomic nuclei of the aluminium. The fraction g of the energy that is converted in such a case is given by

$$g = 2 \cdot 10^{-4} \cdot Z \cdot E_{\beta,max}, \tag{7}$$

with $E_{\beta,max}$ the maximum energy of the β-particles (in MeV) and Z the atomic number of the material where the slowing down occurs.

Expected dose

Risk of exposure comes from 1.83 MeV, 545 keV β^+ particles and 1.275 MeV γ-radation. To determine the risk of exposure from β-radiation, the range of the β particles in aluminium is determined with:

$$R_{\beta,\text{lin.}} = \frac{0.5 E_{\beta,\text{max}}}{\rho},$$

with $R_{\beta,\text{lin.}}$ in cm, E in MeV and ρ is density of the surrounding material in g·cm^3. Aluminium has a density of 2.70 g·cm^3 and $E_{\beta,\text{max}}$ = 1.83 MeV, this gives a range $R_{\beta,\text{lin.}}$ = 0.34 cm. The aluminium surrounding the ^{22}Na is has a thickness of 4 mm, thus there is no risk of direct exposure from β-radiation.

Another risk is Bremsstrahlung. For the experiment, Z = 13 and $E_{\beta,max}$ = 1.83 MeV, it then follows equation 7 that $g \approx 0.005$. The converted energy is then equal to $0.005 \cdot 1.83$ MeV $\approx$ 8.7 keV. Approximately 0.06% of the activity belongs to β^+ decay with an energy of 1.83 MeV, meaning that on average the Bremsstrahlung is $8.7 \cdot 0.5 \cdot 0.0006 \approx 2.6$ eV $\cdot$ s^{-1}, which is negligible and poses no risk.

Tabel 1 and 2 show some relevant values for the source.

Table 1: ^{22}*Na source properties*

Property	Value
Γ	$3.3 \cdot 10^{-13}$ Gy·m^2·Bq^{-1}·h^{-1}
A	0.5 MBq

Table 2: *Setup properties*

Property	Value
μ	0.6452 cm^{-1}
d	0.05 m
r	0.5 m

Filling these values in equations 5 and 6 gives the equivalent dose: $H_T \approx 6.4 \cdot 10^{-1}$ pSv·h^{-1}. There will be two measurements, each with an attendance duration of 3 hours. Thus the total equivalent dose will be 6 $H_T = 3.8$ pSv. This is well below the maximum allowed dose for a student (6 mSv/year), or the effective dose for Dutch citizens (2.4 mSv/year) [5].